

This article was downloaded by:

On: 22 January 2011

Access details: *Access Details: Free Access*

Publisher *Taylor & Francis*

Informa Ltd Registered in England and Wales Registered Number: 1072954 Registered office: Mortimer House, 37-41 Mortimer Street, London W1T 3JH, UK



The Journal of Adhesion

Publication details, including instructions for authors and subscription information:

<http://www.informaworld.com/smpp/title~content=t713453635>

Interphase Formation and the Characterisation of Polymer/Ceramic Adhesion

A. M. Taylor^a; J. F. Watts^a; H. Duncan^b; I. W. Fletcher^c

^a Department of Materials Science and Engineering, University of Surrey, Guildford, Surrey, UK ^b ICI Chemicals & Polymers Ltd., Runcorn, Cheshire, UK ^c ICI Wilton Research Centre, Middlesbrough, Cleveland, UK

To cite this Article Taylor, A. M. , Watts, J. F. , Duncan, H. and Fletcher, I. W.(1994) 'Interphase Formation and the Characterisation of Polymer/Ceramic Adhesion', *The Journal of Adhesion*, 46: 1, 145 – 160

To link to this Article: DOI: 10.1080/00218469408026656

URL: <http://dx.doi.org/10.1080/00218469408026656>

PLEASE SCROLL DOWN FOR ARTICLE

Full terms and conditions of use: <http://www.informaworld.com/terms-and-conditions-of-access.pdf>

This article may be used for research, teaching and private study purposes. Any substantial or systematic reproduction, re-distribution, re-selling, loan or sub-licensing, systematic supply or distribution in any form to anyone is expressly forbidden.

The publisher does not give any warranty express or implied or make any representation that the contents will be complete or accurate or up to date. The accuracy of any instructions, formulae and drug doses should be independently verified with primary sources. The publisher shall not be liable for any loss, actions, claims, proceedings, demand or costs or damages whatsoever or howsoever caused arising directly or indirectly in connection with or arising out of the use of this material.

Interphase Formation and the Characterisation of Polymer/Ceramic Adhesion*

A. M. TAYLOR and J. F. WATTS**

*Department of Materials Science and Engineering, University of Surrey,
Guildford, Surrey, GU2 5XH, UK*

H. DUNCAN

ICI Chemicals & Polymers Ltd., P.O. Box 8, The Heath, Runcorn, Cheshire, WA7 4BD, UK

I. W. FLETCHER

*ICI Wilton Research Centre, P.O. Box 90, Wilton, Middlesbrough,
Cleveland, TS6 8JE, UK*

(Received November 27, 1992; in final form March 1, 1993)

The adhesion of photocured resins to ceramic substrates has been investigated using a variety of surface analytical techniques. Work has been aimed at establishing the physical and chemical interactions between resin and substrate in the interphase region and the effect of environmental exposure on these. Analysis was aided by use of specially-designed, *in-situ* fracture facilities attached by an X-ray photoelectron spectrometer. Specific attention was focused on identification of localised regions of varying chemical composition in adhesive and adherend by imaging spectroscopies (imaging XPS and ToF SIMS imaging) and the study of the significance of such heterogeneities on adhesion and subsequent failure mechanisms.

KEY WORDS polymer/ceramic adhesion; photocured polymer; alumina; XPS; *in-situ* fracture; ToF SIMS; microelectronics; locus of failure; failure mechanisms.

INTRODUCTION

Ceramic substrates, most notably alumina, have found increased use within the electronics industry, particularly in the area of surface mount technology. Alumina substrates can be mass produced at competitive prices and offer the additional advantages of high insulation resistance and low moisture absorption deterioration.¹

*Presented at the International Symposium on "The Interphase" at the Sixteenth Annual Meeting of The Adhesion Society, Inc., Williamsburg, Virginia, U.S.A., February 21–26, 1993.

**Corresponding author.

The upward trend in the use of ceramic materials within the field of electronics has stimulated interest from adhesives manufacturers in developing products suitable for applications such as screen printing and device encapsulation.

Visible light curing resins, (e.g. ICI's Luxtrak™ product range), provide an example of one class of products currently available for use in this area. The light-cured resins are derived from aromatic methacrylate oligomers based on non-epoxy chemistry. The properties which make them of particular interest in such applications include rapid cure times (in a matter of seconds). Cure is initiated by visible light of wavelength 470 nm. The curing radiation used transmits well through alumina and other translucent materials² such that it is possible to cure through 4 mm of alumina ceramic in one minute. The ability to cure the resins with visible light rather than other forms of radiation (e.g. ultraviolet, UV), avoids the possible danger of physiological harm to operators which may result from repeated use of high-intensity ultraviolet radiation.

Electronics manufacturers set rigorous standards of environmental stability, for both exposure to moisture and thermal shock, which all potential adhesives/encapsulants must pass before being accepted into this highly competitive market. Hence the need for full characterisation of the adhesion and failure mechanisms operating within this system.

The work described in this paper has aimed at establishing the physical and chemical interactions that occur between resin and substrate in the interphase region and the effect of subsequent environmental exposure on these. Preliminary work concentrated on the use of surface spectroscopic techniques, (XPS and Static SIMS). The development of *in-situ* fracture facilities for the X-ray photoelectron spectrometer enabled specimens to be fractured in vacuum, then analysed, thus avoiding contamination by air, and the concomitant problem of resolving the contribution to the C1s spectrum of the ubiquitous "contaminant" layer from that of the organic resin. Subsequent studies focused on attempts to identify localised regions of varying chemical composition with the aid of imaging spectroscopies, (imaging XPS and ToF SIMS imaging).

Detailed studies of the composition of sintered alumina products, similar to those investigated here, have revealed the presence of heterogeneities at the surface, caused by migration of magnesium species during the sintering process.^{3,4} The existence of local variations in the surface chemistry has an important bearing on interface chemistry, as their presence could significantly alter the expected interfacial properties. In order to tailor a resin to give optimum durability and strength employed with a particular substrate, it is essential that the surface composition of the substrate be defined as accurately as possible. This enables the formulation chemists to take advantage of such information and define a system capable of promoting durable bond formation, such as acid-base interactions,⁵ across the interface to produce a more stable "interphase region." The importance of acid-base interactions in polymer/ceramic adhesion has previously been emphasised by researchers at IBM in the U.S.A.⁶

Finally, the use of scanning electron microscopy was employed to complement the surface spectroscopic studies in order to study possible correlations between changes in surface morphology and chemical composition.

EXPERIMENTAL

A standard alumina employed in the electronics industry, Coors AD96 (alumina content nominally 96%) was obtained from the Laser Cutting Company in the form of discs, 10 mm in diameter and 1 mm thick. Other than a water rinse following the laser-cutting process, the alumina discs underwent no subsequent cleaning process. This was in order to reproduce most accurately the manufacturing conditions in which Coors AD96 alumina is used by the electronics industry. Luxtrak™ resins were supplied by ICI Specialties. The “as received” materials were characterised using a variety of techniques. SEM micrographs were obtained using a Cambridge Instruments Stereoscan 250, after previously sputter-coating with a layer of gold.

XPS spectra were recorded using a VG Scientific ESCALAB MKII system (with a twin anode capable of supplying either AlK α or MgK α radiation); using analyser pass energies of 50 eV (for survey spectra) and 20 eV (for high resolution spectra). Particular attention was devoted to obtaining good high resolution spectra for the carbon 1s region of the polymer; monitoring the chemical shift on the C1s electrons is an established means of obtaining information relating to the polymer structure.⁷ To aid in this process, a spectrum for the resin was also obtained using the Scienta ESCA300, a spectrometer capable of achieving extremely high spectral resolution, even on insulating samples⁸ (resolution typically of <1.0 eV for the major component of the carbon 1s peak).

Imaging XPS was carried out at ICI Wilton on a VG Scientific ESCASCOPE, using AlK α radiation (1486.6 eV); the analyser was operated in the constant retard ratio (CRR) mode with a value of 4.

Static SIMS spectra were obtained from a VG Scientific ToF SIMS system, with a Reflectron-type analyser and a 30 kV gallium source. All spectra were recorded with the ion gun operating in the synchronous mode at a frequency of 10 kHz and a pulse of 25 ns. ToF SIMS imaging was carried out on the same instrument. The surface charge was neutralised with a pulsed electron gun.⁹

Preparation of Samples for In-Situ Fracture

Coors AD96 alumina discs (as supplied by the Laser Cutting Company) were glued to standard ESCALAB stubs (used for mounting samples in the spectrometer) with high shear strength Araldite™ adhesive, in order to form the separate halves of the joint. A rig was designed for the production of simple butt joints, to prevent misalignment of the joint during cure. The two halves of the joint were secured in the rig and the gauge set to zero. One half of the joint was removed and the Luxtrak™ photocuring resin applied directly to it from a syringe. The joint halves were resecured, with the photocuring resin now sandwiched in between, and the joint was cured under a bifurcated lamp which emitted light of wavelength 470 nm. A gauge was incorporated to allow accurate measurement of the glue-line thickness. Knowledge of this particular parameter is essential in the testing of butt-joints, as the joint strength is inversely proportional to the thickness of the glue.¹⁰ Fully-cured joints were immersed in water at 50°C for varying periods (0–7 days), before being fractured in the ESCALAB preparation chamber using an extensively modified VG

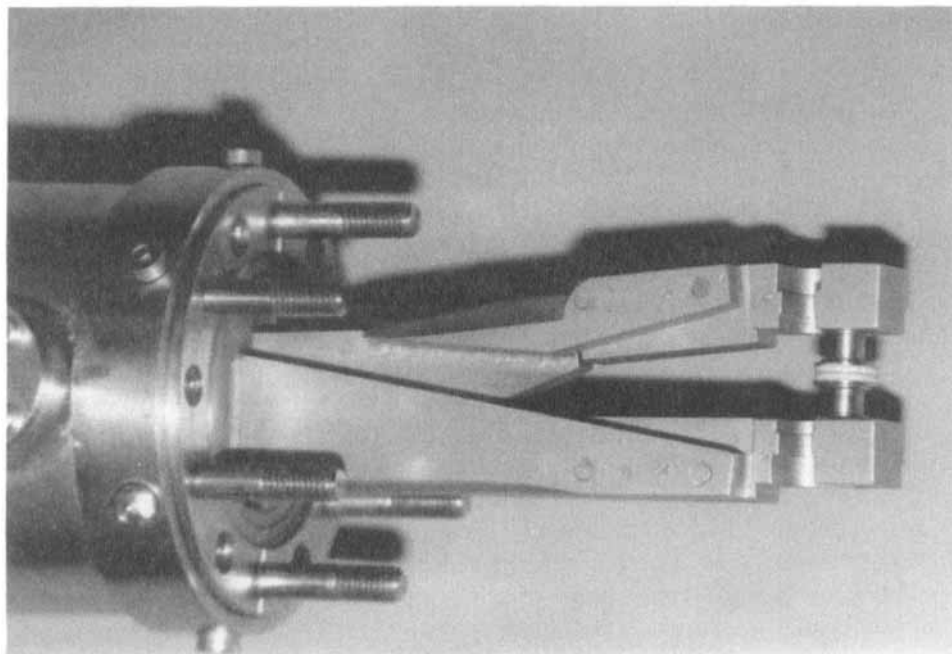


FIGURE 1 Modified T-peel stage for *in-situ* fracture. Shown in horizontal position, it is installed on the preparation chamber of the XPS system in a vertical orientation.

Scientific T-peel stage, as illustrated in Figure 1. As neither the ESCASCOPE nor the ToF SIMS instruments possessed *in-situ* fracture facilities, samples were fractured externally, in the same manner (*i.e.* nominal tension) and loaded into the spectrometers as quickly as was practicably possible.

RESULTS

SEM identified major differences in the fracture surface morphology of samples exposed to various conditions. "Dry joints" failed in a manner analogous to that of an amorphous polymer below its glass transition temperature, *i.e.* conchoidally, Figure 2(a). Failure is believed to have initiated somewhere in the mirror zone. Tear lines (or river lines), point back towards the mirror zone and can be seen at high magnification in the SEM micrograph Figure 3(a). More detailed study of the mirror zone itself using SEM revealed that failure within this region was apparently adhesive, while the remaining fracture surface clearly failed cohesively. Mirror zones produced by the fracture of amorphous polymer or glass rods reflect light specularly.¹¹ In this particular case, the term "mirror zone" refers to the region where fracture appears to have initiated, even though its appearance is not specular in nature; however, the term is employed for consistency of nomenclature. Joints immersed in water at 50°C for less than 7 days displayed a mixed mode of failure. Patches of polymer remained on both surfaces in addition to exposed areas of alumina, apparently free from polymer debris (Fig. 2(b)). Immersion in water for in excess of 7 days led to interfacial failure Figure 2(c), later verified by XPS. SEM

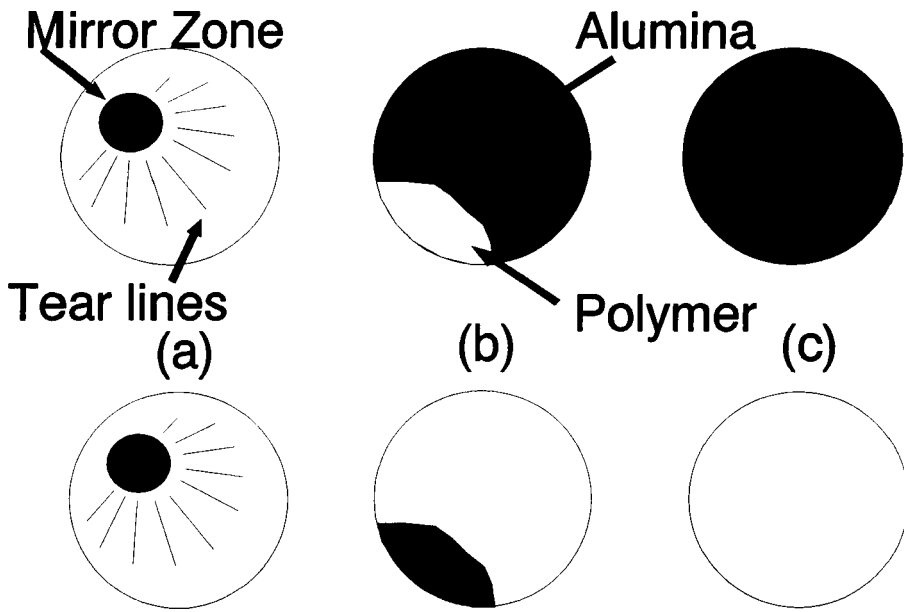


FIGURE 2 Failure modes operating, (a) conchoidal, (b) mixed and (c) interfacial.

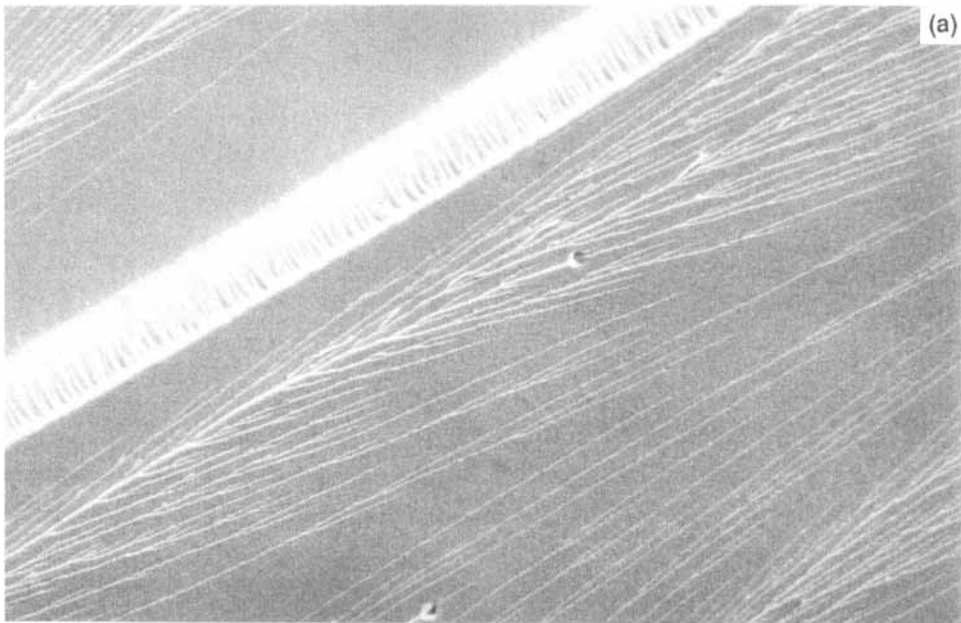


FIGURE 3 SEM micrographs of (a) tear lines on a conchoidal fracture surface; (b) and (c), the two sides of an interfacial failure.

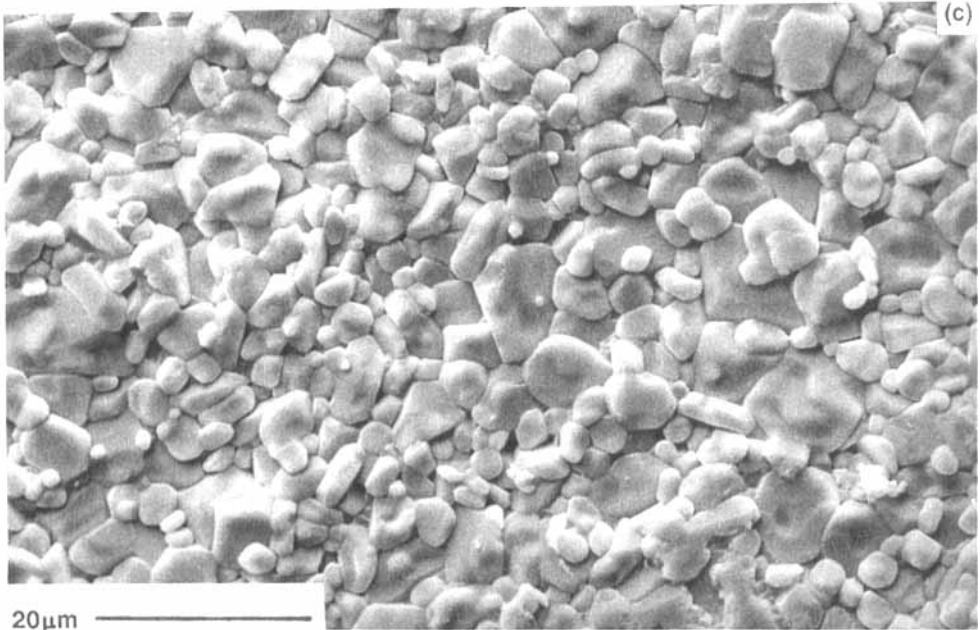
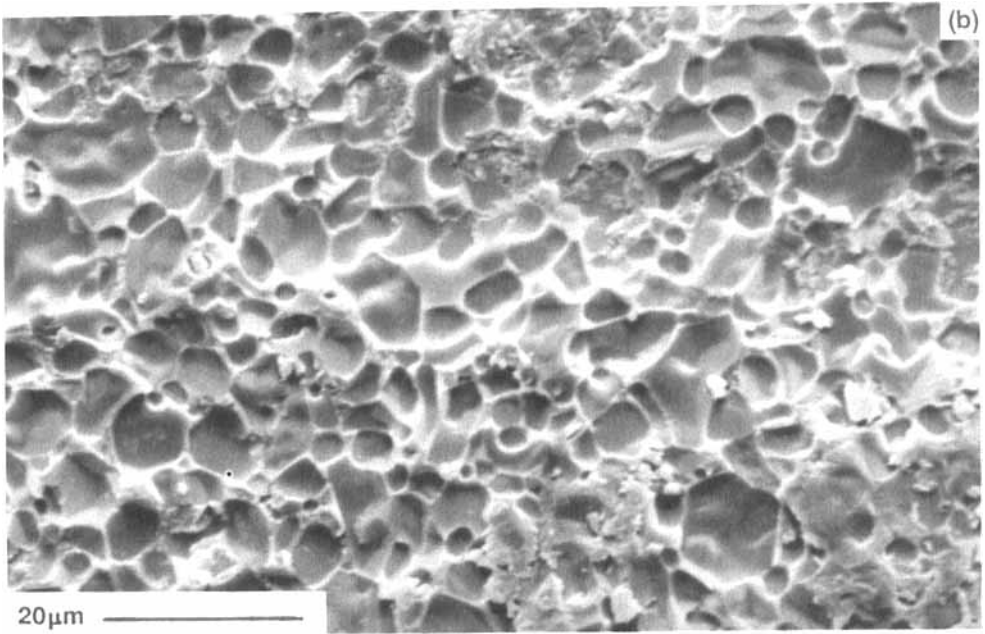


FIGURE 3 (Cont.)

Downloaded At: 13:07 22 January 2011

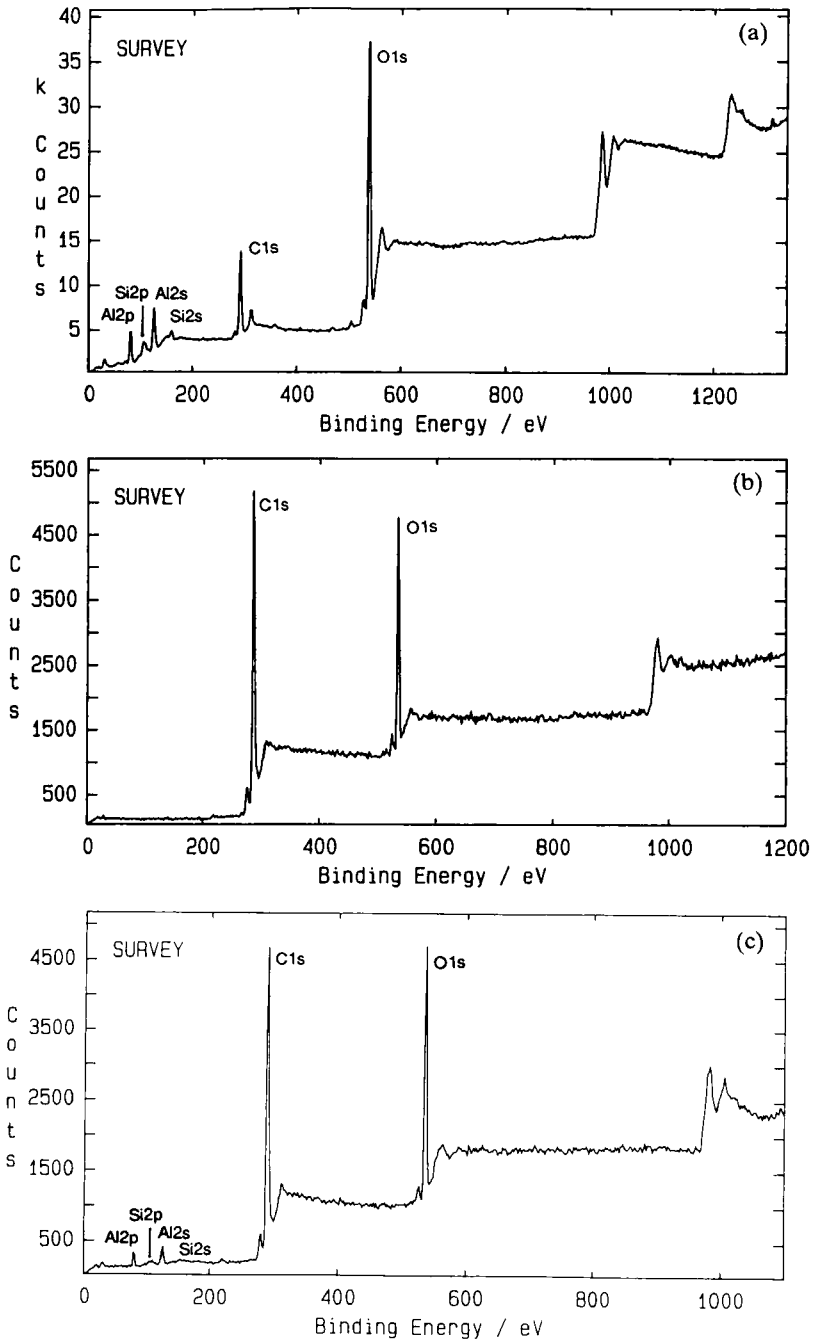


FIGURE 4 XPS survey spectra for (a) as-received Coors AD96 alumina, (b) fully cured resin and (c) conchoidal fracture surface.

studies indicated the operation of markedly different failure mechanisms, as illustrated in the SEM micrographs of Figures 3(b) and (c). These variations in failure mode after environmental exposure one readily appreciates from the schematic illustrations of Figures 2(b) and (c), compared with that of the dry joint of Figure 2(a).

Analyses of the surface composition of as-received alumina, together with fully-cured resin, were carried out by XPS, Figures 4(a) and (b). High resolution spectra were also obtained for the carbon 1s region of the polymer; Figures 5(a) and (b) compare the narrow scans obtained from the ESCALAB MKII and Scienta ESCA300 spectrometers, respectively. Although the peak widths vary considerably, due to the superior spectral resolution of the Scienta ESCA300 the positions of the singlet peaks are in close agreement (Table I). As a result of this, there is now more confidence in the protocol developed for peak-fitting data obtained on the ESCALAB MKII.

XPS was also able to confirm that prolonged immersion (greater than 7 days) in warm water results in interfacial failure. One-half of the joint produced an XPS spectrum which matched that obtained for the as-received polymer and the other half produced a spectrum which resembled, but was not identical to, the result from the Coors AD96 alumina disc. The as-received alumina surface has a significant level of adventitious carbon present, as seen in the survey spectrum of Figure 6(a) and the quantitative data of Table II. The C1s spectrum from this sample is apparently a singlet with a peak width of 2.2 eV. This feature is characteristic of substrates used in technological applications, with a medium-to-high level of hydrocarbon contamination which will dominate any minor contribution from polar carbon that may be present.¹² On failure of the specimen immersed in water, a different result was observed to that described above for the as-received ceramic. The spectrum from the alumina side of the joint indicates a slight reduction in surface carbon concentration but, more significantly, a broadening of the C1s spectrum as seen in Figure 6(b). This observation we attribute to the presence of polar carbon (previously lying adjacent to the alumina surface and obscured by the main hydrocarbon peak of the adventitious layer),¹³ which subsequently reoriented itself closer to the hydrocarbon contamination/Luxtrak™ interface. It is not considered to be a consequence of a thin overlayer of the Luxtrak™ polymer under investigation, which exhibits a very characteristic spectrum, as described in the data in Figure 5.

TABLE I
Comparison of ESCALAB MKII and Scienta ESCA300 data for fully cured Luxtrak™ resin

Component	Scienta ESCA300 data			ESCALAB MKII data		
	Centre (eV)	FWHM (eV)	Area (%)	Centre (eV)	FWHM (eV)	Area (%)
1. C—C/C—H	285.0	1.14	64.0	285.0	1.91	67.0
2. C—O	286.4	1.50	25.9	286.6	2.05	25.0
3. C=O	289.1	1.16	6.2	289.1	1.66	6.0
4. $\pi - \pi^*$	291.8	2.00	3.8	291.7	2.16	3.0

*Data for central positions of peaks has been normalised so that the C—C peak lies at 285.0 eV.

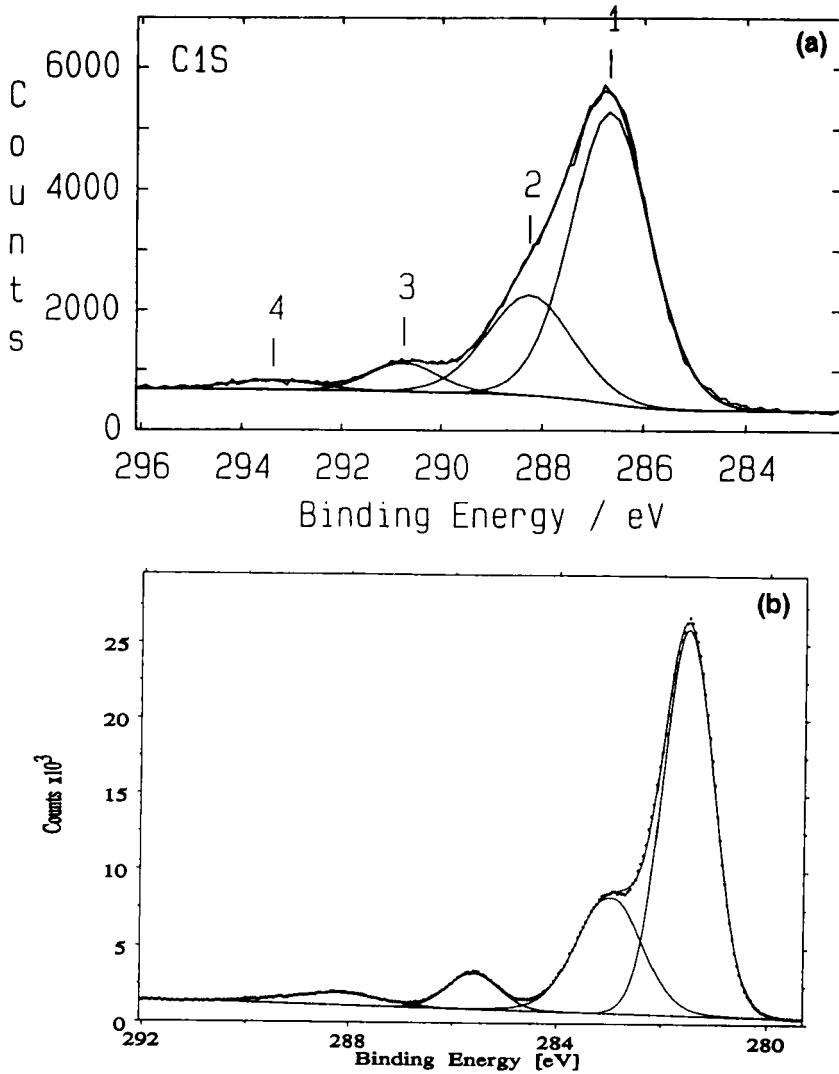


FIGURE 5 Comparison of C1s spectra of photocured polymer obtained with (a) VG Scientific ESCALAB MKII and (b) Scienta ESCA300 spectrometers. FWHM of the major component of each spectrum is 1.91 and 1.14 eV, respectively.

TABLE II
Surface chemical compositions of (a) as-received alumina, (b) alumina side of a joint which failed interfacially and (c) as-received Luxtrak™ resin

Sample	Surface composition (atomic %)			
	Al (2p)	Si (2p)	C (1s)	O (1s)
As-received Coors AD96 alumina	19.4	4.6	43.8	32.2
Alumina side of interfacial failure	20.3	3.9	46.2	29.6
Fully cured LCR000 resin	0	0	84.	15.

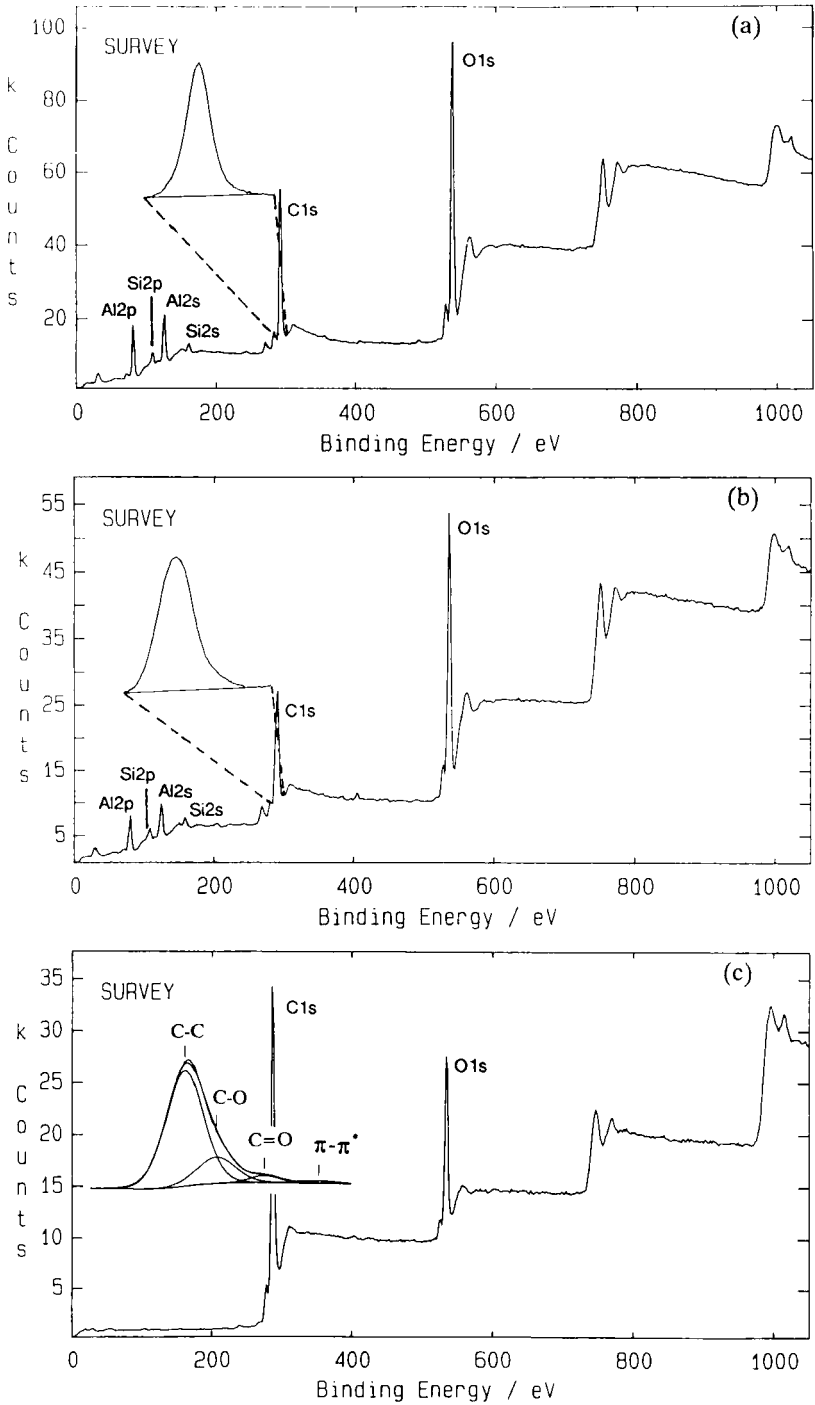


FIGURE 6 Comparison of both survey and C1s spectra for (a) as-received Coors AD96 alumina, (b) alumina side of an interfacial failure and (c) Luxtrak™ side of the interfacial failure.

Downloaded At: 13:07 22 January 2011

These data are consistent with failure occurring at the junction of, or just within, an adventitious layer which exists on the alumina substrate prior to bonding and is slightly rearranged during the cure of the polymer. The latter is most likely and is suggested by curve-fitting the C1s spectrum. This indicated a relative increase in the C—H contaminant, most likely arising from a thin layer of adventitious material which became transferred to the polymer side of the interfacial failure.

However, when SEM micrographs and XPS data from the fracture surface of a “dry” joint were studied, a discrepancy was noted. SEM had revealed a distinct region apparently devoid of polymer (mirror zone in Fig. 2(a)). This was not evident from the XPS spectrum of the same surface, Figure 4(c). The two possibilities that exist to account for this are firstly, that there was a very thin (approximately 10 nm) layer of polymer on the alumina or, alternatively, the contribution from this region relative to that of the total spectrum was not discernible. Standard XPS is an “area averaging” technique, sampling an area of about 10 mm² and, as such, is unable to provide spatially-resolved information. In order to resolve chemical differences within specific features, imaging XPS, with a spatial resolution of 10 μm, was used.

Imaging XPS indicated that the mirror zone of the conchoidal fracture surface had no overlying polymer on it, as SEM results had suggested, *i.e.* failure in this region was adhesive, while the region outside this zone (river lines) failed cohesively. The image in Figure 7 was obtained by mapping the Al2p and C1s signals, having previously corrected for electrostatic sample charging.

Static SIMS spectra obtained from the surface of an as-received Coors AD96 alumina disc revealed the presence of species other than those associated with a sample of pure alumina, Figure 8. Magnesium and calcium were detected at the surface and these species are a result of the sintering aids added during the manufacturing process, which include silica, magnesium oxide and calcium oxide. The distri-

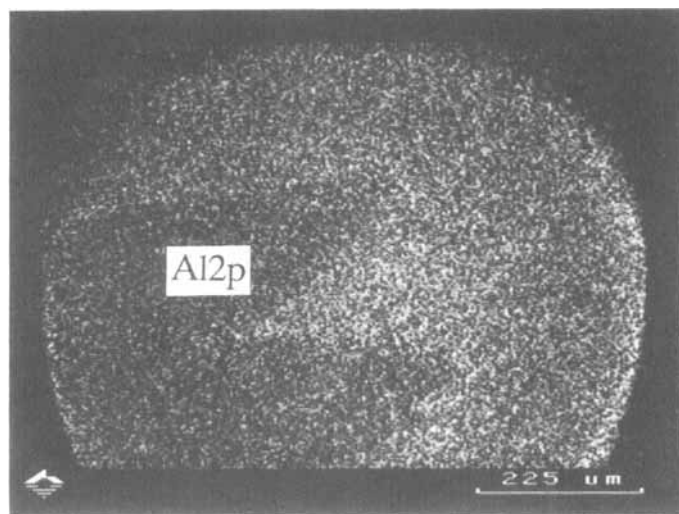


FIGURE 7 Mirror zone edge, obtained by imaging XPS.

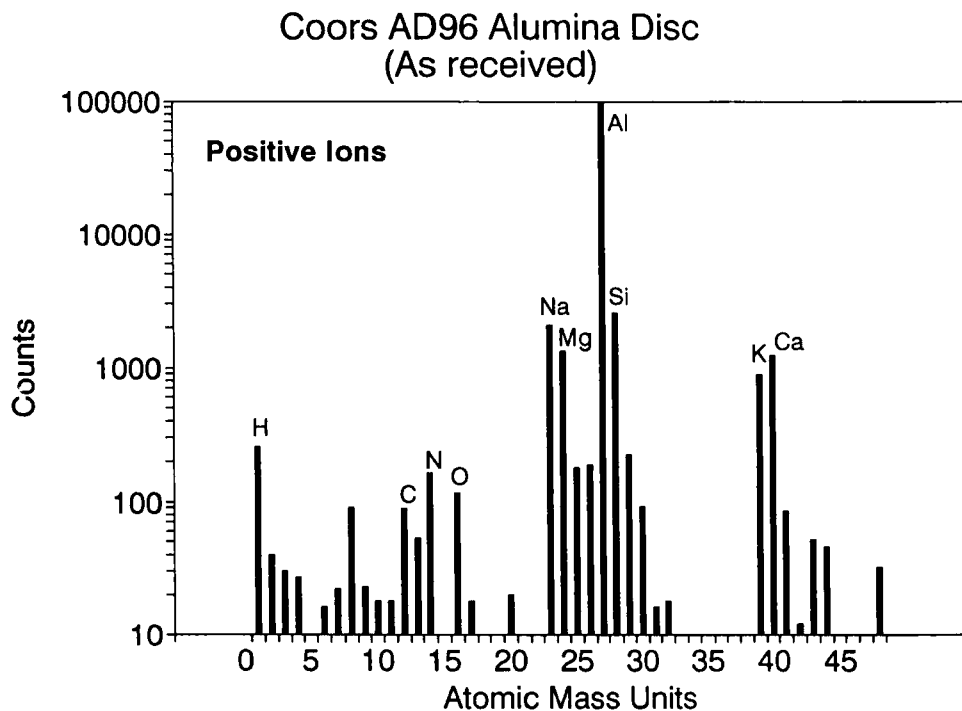


FIGURE 8 Positive ToF SIMS spectrum of a Coors AD96 alumina disc.

bution of these additions is of primary interest in this work, prompting the use of ToF SIMS imaging.

ToF SIMS imaging has been used to study lateral inhomogeneities in the chemical composition of the alumina substrate which alter the bonding character of the joint. As with imaging XPS, the edge of a mirror zone from a conchoidal fracture was chosen for study. Selecting three mass "windows," 128×128 pixel images were collected. Figure 9(a) depicts a primary-ion-induced SEM image of the area under observation. The dark grey area to the left belongs to the mirror zone and the lighter grey area to the polymer. In the secondary ion maps for Mg, Al and Ca, Figures 9(b)–(d), the darkest areas correspond to the polymer regions. The entire "rough" area in Figure 9(a) is the mirror zone where the Mg, Al and Ca are exposed. A slight enhancement in the magnesium signal (marked "M") was observed, Figure 9(b), while a stronger calcium signal was also noted in Figure 9(d), (marked "C"). This demonstrates the presence of local variations in the surface chemistry, which clearly warrant further investigation.

DISCUSSION

A combined study of the spectroscopic and microstructural information obtained from this system has enabled an adhesion failure mechanism to be postulated, for

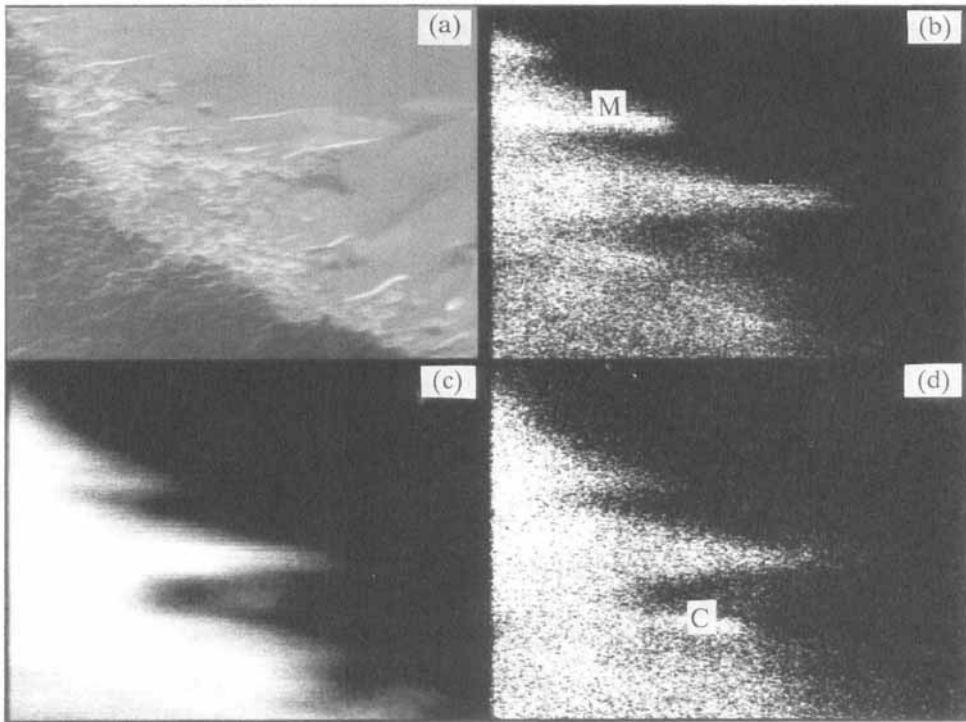


FIGURE 9 ToF SIMS image (a) primary ion induced electron image, (b) magnesium map, (c) aluminium map and (d) calcium map.

joints which have not been subject to environmental attack. Initially, there was some uncertainty as to whether or not the resin wet the surface of the alumina completely. SEM micrographs taken from a sample of resin cleaved from an alumina strip, revealed a surface morphology which replicated the granular structure of the ceramic,¹³ suggesting that the resin does indeed wet the alumina surface. Butt joints fractured in simple tension failed in a manner likened to the conchoidal fracture surfaces observed when glass or amorphous polymers undergo brittle failure. Figure 10 is a schematic of the main features present on such fracture surface; the SEM micrographs, Figures 10(a)–(d), depict the detailed surface morphology within those regions. The point of failure initiation is generally located within the mirror zone, so the observation of a defect within that region would be an important result. Figure 10(b) is an SEM micrograph of what appears to be a bubble, perhaps trapped in the resin during joint production. Figure 11 illustrates the possible case of a bubble acting as a stress raiser, causing failure to initiate. It should be noted that, although the joint was loaded in simple tension (otherwise known as Mode I failure), the problem is more complex and any slight misalignment in specimen loading can induce an element of shear (Mode II failure). Variation in the elastic properties across a bimaterial interface also introduces shear forces. Bimaterial interfacial fracture is, therefore, controlled by the relative amounts of mode I and II forces operating.¹⁴

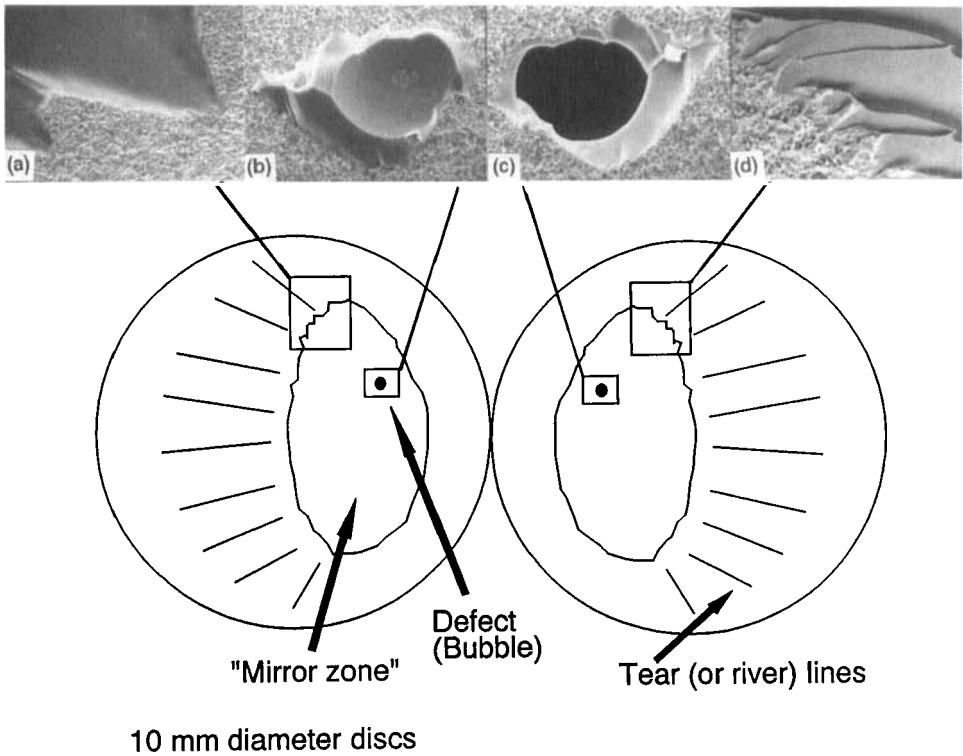


FIGURE 10 Schematic of a conchoidal fracture surface with SEM micrographs depicting the detailed surface morphology.

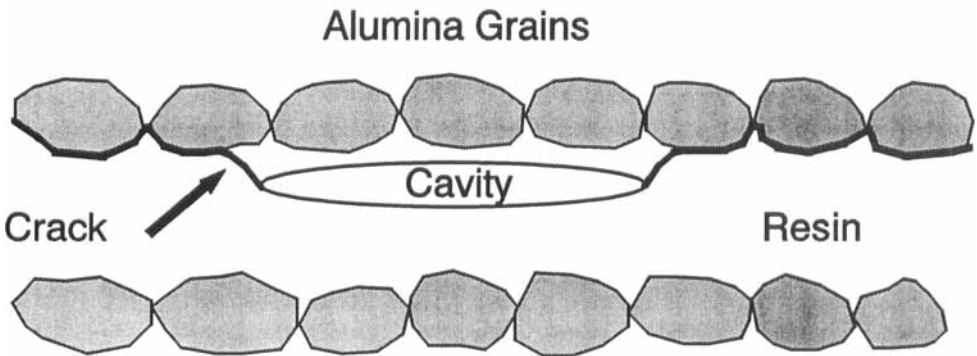


FIGURE 11 Fracture initiation by a defect (bubble or cavity).

Downloaded At: 13:07 22 January 2011

In this particular case, it is suggested that a physical defect, most likely a gas bubble, or polymer cavity, is responsible for crack initiation. Other potential sites include areas of lower polymer cross link density or regions of chemical heterogeneity. Failure within the mirror zone was confirmed as interfacial by both SEM and imaging XPS. A more detailed study of the mechanical properties of this system,¹⁴ involving the use of double cantilever beam tests (pure Mode I failure), also resulted in interfacial failures. XPS carried out on the underside of the polymer, which had previously been adhered to the alumina, did not reveal the presence of inorganic material. This makes it unlikely that the instability of the interface is due to the presence of a weak boundary layer resulting from the presence of surface-segregated processing aids.

The remaining area of the conchoidal fracture surface failed cohesively. It had previously been observed that an interfacial crack between photocured polymer and glass could become energetically unstable,¹³ so it was not surprising to find the crack front move away from the interface and travel through the polymer for the latter part of its route.

It is, therefore, possible to summarise the various stages of the failure mechanism for the fracture of a butt joint in simple tension:

- (i) A crack is initiated at a defect, in this case a bubble.
- (ii) The crack runs interfacially for a certain distance. At this stage, the crack is forced to change direction continually as it follows the natural contours of the alumina grains.
- (iii) Eventually, the crack becomes unstable and follows an energetically more favourable pathway within the polymer itself.

At this stage, it is not possible to discuss a detailed failure mechanism for joints which have been exposed to water. SEM studies coupled with XPS have revealed an interfacial mode of failure, but it is unclear whether water ingress occurs along the interface or through the bulk of the polymer. The observation of a true interfacial failure is rare and is also in contrast to other work on the adhesive bonding of aerospace materials, where a thin layer of polymer (1–2 nm thick) remains on the substrate.^{15,16} In order to ascertain the mechanism by which exposure to water leads to interfacial failure (*i.e.* does the water simply displace the polymer or is it first plasticised), future work will attempt to monitor the precise route by which water ingress occurs, and the orientation of organic molecules at the inorganic surface.

CONCLUSIONS

XPS is a very effective means of characterising surface compositions. Coupled with *in-situ* fracture facilities, it may also be used to identify loci of failure in an adhesive joint. However, in order to ascertain more precisely the failure initiation site, and/or potential sites for primary bonding, techniques capable of providing spatially-resolved information must be used, *i.e.* imaging XPS and ToF SIMS imaging.

Various failure mechanisms have been shown to operate in this particular system,

depending upon the sample history (*i.e.* exposure to moisture or a dry environment). ToF SIMS imaging has revealed local variations in the surface chemistry of the alumina. In the case of “dry” joints, the presence of these chemical heterogeneities appears to be overshadowed by the existence of much larger defects, *i.e.* bubbles or cavities, which act as failure initiation sites. The extent to which variations in surface chemistry may contribute to the failure mechanism of samples immersed in water is at this stage unclear and will be investigated further.

Acknowledgements

The financial support of both ICI Chemicals & Polymers Ltd. and the SERC is gratefully acknowledged by AMT. for their funding of this CASE award. Special thanks go also to A. M. Brown, S. J. Greaves and M. P. Hill for technical advice and informative discussions.

References

1. T. Ueyama and H. Wada, *Advanced Ceramics*, 2nd ed. (Oxford University Press and Ohmsha Ltd., 1988), Chap. 10, pp. 184–199.
2. S. C. Rogers, *Adhesives Age*, April, (1988).
3. R. I. Taylor, J. P. Coad and R. J. Brook, *J. Am. Ceram. Soc.* 539–540 (1974).
4. D. R. Clarke, *J. Am. Ceram. Soc.*, 339–341 (1980).
5. D. M. Brewis and D. Briggs, *Industrial Adhesion Problems* (Orbital Press, Oxford, UK, 1985), Chap. 3, pp. 66–68.
6. T. S. Oh, L. P. Buchwalter and J. Kim, *J. Adhesion Sci. Technol.* **4**, 303–317 (1990).
7. J. F. Watts, *An Introduction to Surface Analysis by Electron Spectroscopy* (Oxford University Press, 1990), Chap. 5, pp. 58–61.
8. G. Beamson and D. Briggs, *High Resolution XPS of Organic Polymers* (John Wiley & Sons, New York, 1992), Chap. 4, pp. 13–17.
9. D. Briggs, M. J. Hearn, I. W. Fletcher, A. R. Waugh and B. J. McIntosh, *Surface and Interface Analysis* **15**, 62–65 (1990).
10. K. Kendall, *Contemp. Phys.* **21**, 277–297 (1980).
11. B. R. Lawn and T. R. Wilshaw, *Fracture of Brittle Solids* (Cambridge University Press, 1975), Chap. 5, pp. 100–103.
12. J. E. Castle and J. F. Watts, *Corrosion Control by Organic Coatings* (NACE, Houston, Texas, 1981), pp. 78–86.
13. A. M. Taylor and J. F. Watts, unpublished study (1991/92).
14. I. Priour, *Study of a Crack Growth along A Polymer-Ceramic Interface*, M.Sc. project, Imperial College of Science, Technology and Medicine, London, UK, (1991/92).
15. J. F. Watts, R. A. Blunden and T. J. Hall, *Surface and Interface Analysis* **16**, 227–235 (1990).
16. J. F. Watts and B. R. Dempster, *Surface and Interface Analysis* **19**, 115–120 (1992).